PROC. OF JSCE
No. 339, November 1983

A STUDY ON LATERAL BUCKLING STRENGTH AND DESIGN AID FOR HORIZONTALLY CURVED I-GIRDER BRIDGES

By Hiroshi NAKAI and Hisao KOTOGUCHI***

1. INTRODUCTION

During the past decade, numerous horizontally multiple curved I-girder bridges have been constructed in the highways of all over the world as pointed out in reference[1], because such types of bridges can easily be designed and fabricated in the case where the span length of a bridge is comparatively short. For example, it is recommended by the bridge structural design code of the Hanshin Highway Public Corporation[2] that multiple curved I-girder bridges should be decided in accordance with their radius of curvature R and span length L as shown in **Fig. 1** through the various parametric studies.

However, the Japanese Specification for Highway Bridges does not provide a criterion for the lateral buckling strength of the horizontally curved I-girder which is adopted as the main girder of the multiple curved I-girder bridges[3]. Therefore, the engineers are always compelled to utilize the criterion for that of the straight girder bridges. There are, accordingly, so many unclarified problems concerning the safety against the lateral buckling strength of a curved I-girder, that it is an important problem to inquire these points extensively.

This paper deals with the experimental and theoretical studies on the lateral buckling behaviours for the curved I-girders, and gives a recommendation to estimate the lateral buckling strength and apply to a rational design for the multiple curved I-girder bridges.

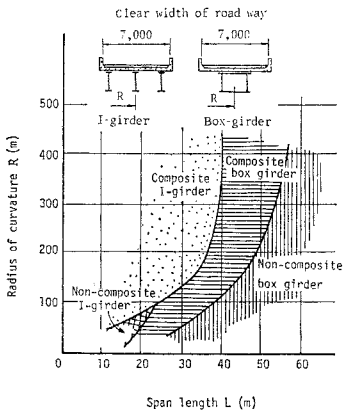

Fig. 1 Adequate type of horizontally curved girder bridges.

* Member of JSCE, Dr. Eng., Professor, Department of Civil Engg., Osaka City University

** Member of JSCE, Dr. Eng., Associate Professor, Department of Construction Engg., Daido Institute of Technology

2. EXPERIMENTS ON LATERAL BUCKLING OF MULTIPLE CURVED I-GIRDER BRIDGES

The lateral buckling behaviours of multiple curved I-girder bridge will distinctly be classified into two categories as follows, i.e. one is the most dangerous phenomenon such as the overall lateral buckling throughout a bridge, and the other is a local one of the main girders between the supporting points alike the floor beams or sway and lateral bracings. In order to clarify these phenomena, a series of experimental studies were conducted prior to the theoretical analyses.

(1) Overall lateral buckling tests of multiple curved I-girder bridges[4]

a) Model girders

Three model girder bridges MG-1, MG-2 and MG-3 with two main I-girders having floor beams and three different lateral bracings were built on the scale 1 : 3.8 based on the dimensional analysis of the actual bridges of the multiple curved I-girder bridges.

Fig. 2 and **Fig. 3** show the plan and the cross-section of model girders, respectively. The ratio between span length L and girder spacing B was equal to $L/B=5.56$. The local buckling of flange

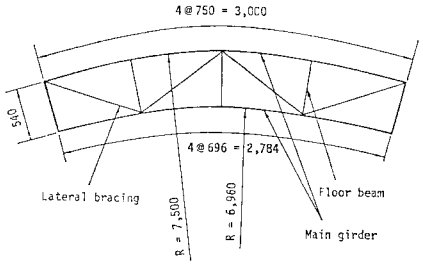

Fig. 2 Plan of model girder (dimension in mm).

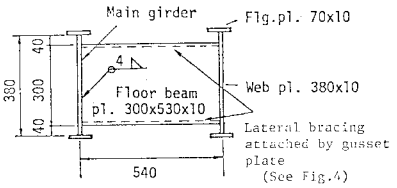

Fig. 3 Cross-section of model girder (dimension in mm).

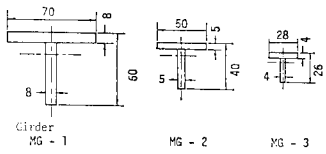

Fig. 4 Cross-section of lateral bracings (dimension in mm).

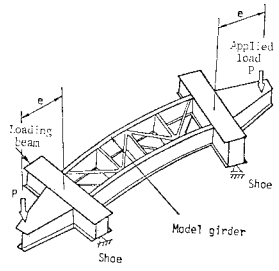

Fig. 5 Loading conditions.

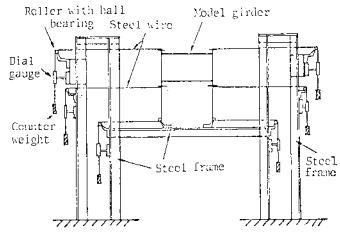

Fig. 6 Measurement of displacements.

and web plates could effectively be prevented by taking their thickness as large as possible.

While, the cross-sections of the lateral bracings of the model girders MG-1, MG-2 and MG-3 were respectively chosen to have twice, one and half times of the cross-sectional area of lateral bracings based upon the dimensional analysis of the actual bridges as shown in **Fig. 4**.

The materials of all these members were made of structural steel SS-41 with the Young's modulus of elasticity $E=2.1\times10^6$ kg/cm² (205.8 GPa), Poisson's ratio $\mu=0.3$ and yield stress $\sigma_y=3\,100$ kg/cm² (303.8 MPa).

b) Loading conditions

It is preferable that the lateral buckling tests should be performed under a condition where the shearing force will not appear as same as pure bending in a straight beam. To satisfy this condition as exactly as possible, two loading beams with cantilever tongues were bolted to the model girder. The upper shoes using the load cell tranceducers were also bolted to these loading beams and the lower shoes were set in order that the model girder was supported on a roller at one end and a pin at the other. And then the same loads P were applied to the ends of cantilevers by the oil jacks as is seen in **Fig. 5**.

Thus, the model girder can approximately be subjected to the pure bending moment $M=P\cdot e$, where e is the eccentricity of the load and the shoe in the direction of the girder axis.

c) Measurements of displacement and strain

The lateral displacements were measured by the special instruments which consist of steel wire ($\phi=0.3$ mm), roller with ball bearing, counter weight (300 gr) and dial gauges with the accuracy 1/100 mm as illustrated in **Fig. 6**.

On the other hand, strains in main girders and lateral bracings were measured by the ordinary electrical wire strain gauges with the gauge length 5 mm and 3 mm for main girder and lateral bracings, respectively.

d) Test results

Fig. 7 shows an example of the load-strain curves for the main girders. The corresponding lateral displacements of the main girders can be plotted as shown in **Fig. 8**.

Observing **Fig. 7**, it is clear that the strain at the point 1 in the cross-section changes from compression to tension when the applied moment reaches a certain value. This bending moment can be considered as lateral buckling moment. And, this moment can be decided by obtaining

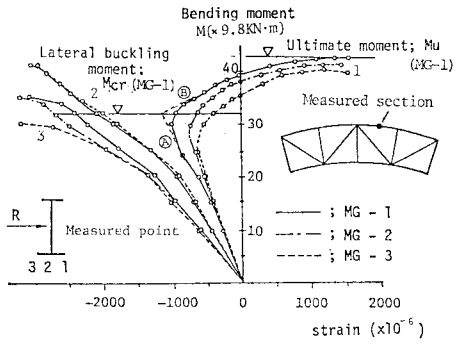

Fig. 7 Load-strain curves (main girder).

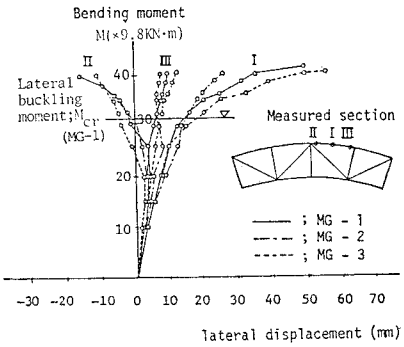

Fig. 8 Load-lateral displacement curves (main girder).

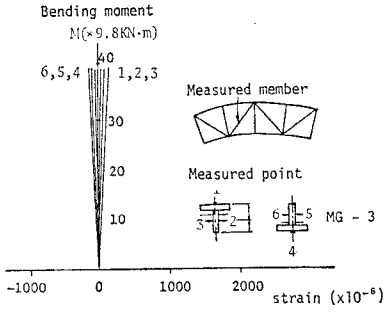

Fig. 9 Load-strain curves (Lateral bracing).

an intersection of the tangents to the load-strain curve at the two points A and B as shown in **Fig. 7**. Thus, the lateral buckling moments M_{cr} and the ultimate moments M_u of girders MG-1 through MG-3 can clearly be obtained and these values can be summarized as shown in **Table 1**.

Table 1 M_{cr} and M_u (Unit: KN·m).

Girder	M_{cr}	M_u
MG-1	303.8	416.5
MG-2	294.0	401.8
MG-3	284.2	392.0

From this table, it seems that both the moments M_{cr} and M_u are not significantly affected by the differences of the lateral bracings, because the strains remain within the elastic ranges even in a case of the minimum cross-sectional area as shown in **Fig. 9**.

The relative lateral buckling displacements at the compression flanges of outer girder of MG-3 for each load steps can be plotted as shown in **Fig. 10** by the subtraction of the absolute displacements at the junction points of floor beams and lateral bracings. Observing this figure, the

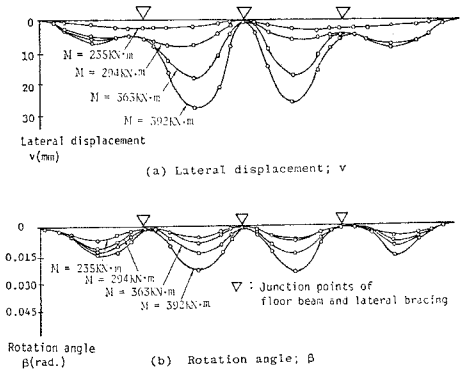

Fig. 10 Lateral buckling modes of outer girder of MG-3.

local lateral buckling modes of the main girder between floor beams and lateral bracings predominate rather than the overall buckling.

In consequence, it is concluded from these facts that the overall lateral buckling of the multiple curved I-girder bridges is not so an important phenomenon that we have to devote our attentions to the local buckling of main girder between the supported portions by floor beams or sway and lateral bracings, if the ratio L/B of span length to girder spacing has a small value, and the floor beams or sway and lateral bracings are designed to have enough strength and rigidity against the lateral loads as described in the preceding section.

(2) Local buckling tests of curved I-girders[5]

The buckling tests for a supported portion of the main girders among the junction points of floor beams and lateral bracings, which is idealized as shown in **Fig. 11**, were undertaken by the similar procedures as mentioned in the above to evaluate the local buckling strength of the main girder. Twenty-seven model girders IG-1 through IG-27 (see **Table 2**) were tested under the loading conditions as illustrated in **Fig. 12**.

Typical load-displacement curves and the lateral buckling modes can be plotted as shown in **Fig. 13** and **Fig. 14**, respectively.

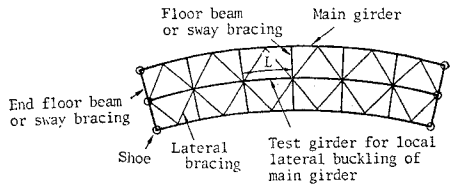

Fig. 11 Detail of multiple curved I-girder bridge.

Table 2 Comparison of ultimate moment M_u.

Item / Girder	Span L (m)	Radius R_s (m)	Central angle (rad.)	Flange area A_f (cm²)	Web area A_w (cm²)	Ultimate moment M_u (kN·m) Ex.	Th.	Ex./Th.
IG-1	2.5	5	0.5	8	38	52.9	58.8	0.90
IG-2	2.5	15	0.17	8	38	86.2	91.1	0.95
IG-3	2.5	30	0.08	8	38	109.8	113.7	0.97
IG-4	2.3	4.6	0.5	18	38	135.2	178.4	0.76
IG-5	2.3	13.8	0.17	18	38	202.9	209.8	0.97
IG-6	2.3	27.6	0.08	18	38	202.9	223.4	0.91
IG-7	1.8	3.6	0.5	20	38	161.7	192.1	0.84
IG-8	1.8	10.8	0.17	20	38	261.7	256.8	1.02
IG-9	1.8	21.6	0.08	20	38	274.4	263.6	1.04
IG-10	0.9	1.8	0.5	20	38	201.9	251.9	0.80
IG-11	0.9	5.4	0.17	20	38	271.5	280.3	0.97
IG-12	0.9	10.8	0.08	20	38	301.8	314.6	0.97
IG-13	2.5	5	0.5	6	38	45.1	35.3	1.28
IG-14	2.5	15	0.17	6	38	65.7	66.6	0.99
IG-15	2.5	30	0.08	6	38	80.4	80.4	1.00
IG-16	2.5	5	0.5	10	38	61.7	89.2	0.69
IG-17	2.5	15	0.17	10	38	113.7	109.8	1.04
IG-18	2.5	30	0.08	10	38	136.2	120.5	1.13
IG-19	2.5	5	0.5	12	38	76.4	115.6	0.66
IG-20	2.5	15	0.17	12	38	139.2	135.2	1.03
IG-21	2.5	30	0.08	12	38	176.4	150.9	1.17
IG-22	2.5	15	0.17	14	38	117.4	156.8	1.13
IG-23	2.5	30	0.08	14	38	193.1	162.7	1.19
IG-24	2.3	4.6	0.5	7	38	51.0	56.8	0.90
IG-25	2.3	13.8	0.17	7	38	80.4	79.4	1.01
IG-26	2.3	27.6	0.08	7	38	100.9	91.1	1.11
IG-27	2.3	∞	0	7	38	146.0	113.7	1.28

Ex.: Experiment, Th.: Theory

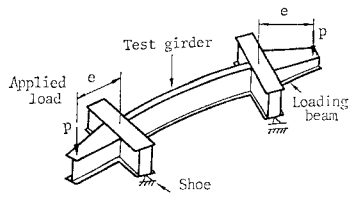

Fig. 12 Loading conditions.

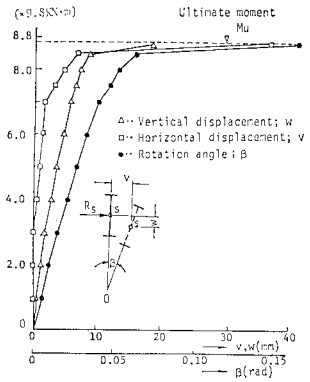

Fig. 13 Load-displacement curves (IG-2).

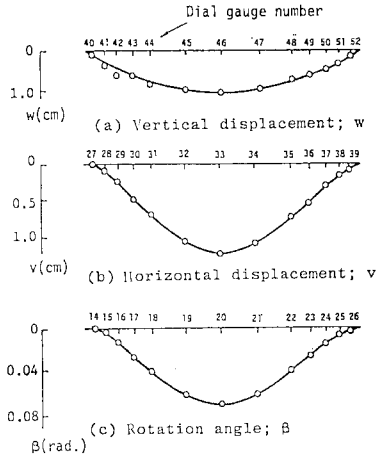

Fig. 14 Buckling modes (IG-2).

3. ANALYTICAL STUDY ON LATERAL BUCKLING OF CURVED I-GIRDERS

(1) Analytical study

The horizontal and vertical displacements and rotation angle of a curved I-beam will occure in a beam even though the applied moment is relatively small. However, once a certain critical moment is reached, the curved beam bows largely out sideways. This bending gives the large displacements which cause a curved I-beam to buckle. A few finite displacement theories, which have been developed by many researchers,[6)~18)] can be used to investigate these complex phenomenon.

However, the material non-linearity will predominate greater than the geometrical one. This tendency can obviously be understood by a survey of the actual curved bridges as shown in **Fig. 15**[14)], and almost all the lateral buckling of I-girders fall within the elasto-plastic regions since the buckling parameters (cf. Eq. (13)) have $\alpha=0.3\sim1.2$[3)].

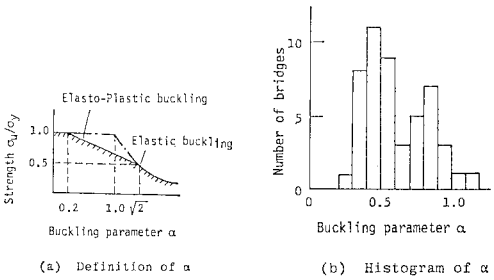

Fig. 15 Lateral buckling parameter α and corresponding buckling behaviours.

Accordingly, this paper deals with the lateral buckling behaviour by the theory based upon second order analysis as pointed out by reference[15)~17)].

For this analysis, if the buckling displacements at the state-2 are assumed in reference to the undeformed state-1 in which the displacements in a beam are assumed to be negligible small until the applied moment reaches a lateral buckl-

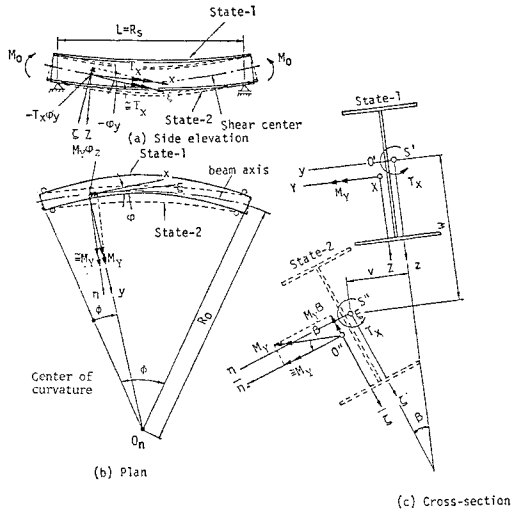

Fig. 16 Buckling displacements and additional stress-resultants.

ing moment, the following relationships between displacements and stress-resultants will be obtained by referring **Fig. 16** with an asymmetrical I-girder[24];

$$\left.\begin{aligned}
&EI_Y\left(\frac{d^2w}{ds^2}-\frac{\beta}{R_s}\right)+EI_{YZ}\left(\frac{d^2v}{ds^2}+\frac{1}{R_s}\frac{du}{ds}\right)=-\frac{R_0}{R_s}M_{\bar{\eta}}\\
&EI_Z\left(\frac{d^2v}{ds^2}+\frac{1}{R_s}\frac{du}{ds}\right)+EI_{YZ}\left(\frac{d^2w}{ds^2}-\frac{\beta}{R_s}\right)=\frac{R_0}{R_s}M_{\bar{\zeta}}\\
&EA_X\left\{\frac{du}{ds}-\frac{v}{R_s}-\left(\frac{d^2w}{ds^2}-\frac{\beta}{R_s}\right)z_s\right.\\
&\quad\left.-\left(\frac{d^2v}{ds^2}+\frac{1}{R_s}\frac{du}{ds}\right)y_s\right\}=\frac{R_0}{R_s}N_{\bar{\xi}}\\
&EI_\omega\frac{d^2\theta}{ds^2}-\overline{GK}\frac{d\theta}{ds}=-T_\xi
\end{aligned}\right\}\quad\cdots\cdots(1)$$

where

s; curvilinear coordinate at shear center

x, y, z; axial, horizontal and vertical coordinate axes at shear center

u, v, w; displacement in the direction of coordinate axes (x, y, z)

$\theta=\beta+w/R_s$; torsional angle ……(2)

β; rotational angle

EI_Y, EI_Z, EI_{YZ}; flexural rigidity with respect to centroidal axes Y, Z, and YZ

EA_X; elongation rigidity

EI_ω; warping rigidity

$$\overline{GK};\ GK+\int_A(y^2+z^2)\sigma dA \quad\cdots\cdots(3)$$

in which

GK; torsional rigidity

$\int_A(y^2+z^2)\sigma dA$; additional torsional rigidity due to the normal stress σ[21]

R_0, R_s; radius of curvature at centroid O' and shear center S'

y_s, z_s; eccentricity between O' and S' in the direction of coordinate axes (y, z)

Now, the additional stress-resultants in the right-hand side of Eq. (1) at state-2 through state-1 will be written as follows;

$$\left.\begin{aligned}
&N_{\bar{\xi}}=0,\quad M_{\bar{\eta}}=-T_x{}^0\varphi_z\\
&M_{\bar{\zeta}}=-M_Y{}^0\beta+T_x{}^0\varphi_y,\quad T_{\bar{\xi}}=M_Y{}^0\varphi_z
\end{aligned}\right\}\quad\cdots(4)_{a\sim d}$$

When girders undergo only the bending moments around the strong axis at the ends of girder $\phi=0$ and $\phi=\Phi$, bending moment $M_Y{}^0$ and torsional moment $T_x{}^0$ at an arbitrary section ϕ will be reduced to;

$$\left.\begin{aligned}
&M_Y{}^0=M_0\cos(\phi-\Phi/2)/\cos\Phi/2\\
&T_x{}^0=M_0\sin(\phi-\Phi/2)/\cos\Phi/2
\end{aligned}\right\}\quad\cdots\cdots(5)$$

Moreover, the warping moment $M_\omega{}^0$ can be given by solving the following equation;

$$\frac{d^2M_\omega{}^0}{ds^2}-\frac{GK}{EI_\omega}M_\omega{}^0=-\frac{M_0}{R_0}\quad\cdots\cdots(6)$$

The deflection angles φ_y and φ_z due to bending can also be found by

$$\varphi_y=-dw/ds,\quad \varphi_z=dv/ds+u/R_s\cdots\cdots(7)_{a,b}$$

Accordingly, substitution of Eqs. (2)~(7) into Eq. (1) gives a set of the simultaneous differential equations for the lateral buckling displacements u, v, w, β and θ as follows;

$$\left.\begin{aligned}
&EI_y\left(\frac{d^4w}{ds^4}-\frac{1}{R_s}\frac{d^2\beta}{ds^2}\right)-\frac{d^2}{ds^2}\left\{T_x{}^0\left(\frac{dv}{ds}+\frac{u}{R_s}\right)\right\}\\
&\quad-\frac{d^2}{ds^2}\left(M_Y{}^0\beta+T_x{}^0\frac{dw}{ds}\right)\frac{I_{YZ}}{I_Z}=0\\
&EI_z\left\{\frac{R_s}{R_0}\left(\frac{d^4v}{ds^4}+\frac{1}{R_s{}^2}\frac{d^2v}{ds^2}\right)+\frac{z_s}{R_0}\left(\frac{d^4w}{ds^4}\right.\right.\\
&\quad\left.\left.-\frac{1}{R_s}\frac{d^2\beta}{ds^2}\right)\right\}+\frac{d^2}{ds^2}\left(M_Y{}^0\beta+T_x{}^0\frac{dw}{ds}\right)\\
&\quad+\frac{d^2}{ds^2}(T_x{}^0\varphi_z)\frac{I_{YZ}}{I_Y}=0\\
&EI_\omega\frac{d^4\theta}{ds^4}-\overline{GK}\frac{d^2\theta}{ds^2}+\frac{d}{ds}\left\{M_Y{}^0\left(\frac{dv}{ds}+\frac{u}{R_s}\right)\right\}=0
\end{aligned}\right\}\quad\cdots\cdots(8)_{a\sim c}$$

where

$$u=\int_0^s v/R_s\,ds+u_0\quad\cdots\cdots(9)$$

u_0: axial displacement at the origin $s=0$ and the symbols I_y and I_z are defined by

$$\left.\begin{aligned}
&I_y=R_s/R_0\cdot(I_Y-I_{YZ}{}^2/I_Z)\\
&I_z=R_s/R_0\cdot(I_Z-I_{YZ}{}^2/I_Y)
\end{aligned}\right\}\quad\cdots\cdots(10)_{a,b}$$

The boundary conditions for displacements and stress-resultants can be put as

$$v=w=\beta=\varphi_z=T_s=0,\quad M_Y=M_0\cdots\cdots(11)_a$$

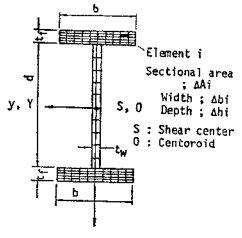

Fig. 17 Segmental method of cross section.

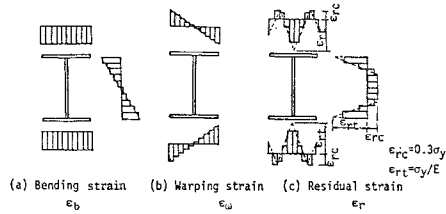

Fig. 18 Strain distribution in I-girder.

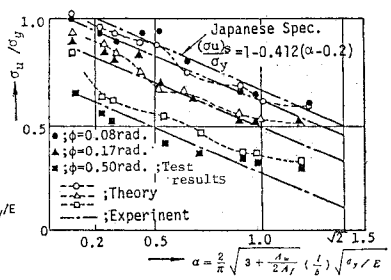

Fig. 19 Lateral buckling strength σ_u.

for both the ends $\phi=0$ and $\phi=\Phi$ of girder, and

$$u=0,\quad N_X=0 \qquad \cdots\cdots(11)_b$$

for $\phi=0$ and $\phi=\Phi$ of girder, respectively.

By the way, these equations coincide perfectly with the results by references 18)~23); provided that the girder is a straight one $R_s=\infty$ having a symmetrical cross-section.

For the analyses of the material non-linearity, a cross-section of girder is divided into the small elements as shown in **Fig. 17**, and the following assumptions are set to estimate the elasto-plastic behaviours for each element;

1. The material obeys the completely elasto-plastic behaviours.
2. Bernoulli-Euler's hypothesis can be applied to both bending strain ε_b $(=M_Y{}^0/EI_Y\cdot Z)$ and warping strain ε_ω $(=M_\omega{}^0/EI_\omega\cdot\omega)$ as illustrated in **Fig. 18** (a) and (b), respectively.
3. The residual stress σ_r distributions are such a pattern as shown in **Fig. 18** (c), in which residual strain means $\varepsilon_r=\sigma_r/E$.
4. The stiffness of element vanishes when the sum of strain ε_b, ε_ω and ε_r exceed the yield strain ε_y $(=\sigma_y/E)$ of materials.

Thus, Eq. (8) can successively be solved by determining the rigidities EI_y, EI_z, EI_{yz} and EI_ω on the basis of the above assumptions by regarding this problem as an eigen-value problem.

(2) Comparison with test results

The numerical calculations were conducted to the test girders IG-1 through IG-27. These results are summarized as shown in **Table 2** together with the experimental ones.

Observing this table, it seems that the theoretical values coincide well with the experimental ones (90%~110%) for the case where the central angle Φ of girder is less than 0.2 rad.

4. LATERAL BUCKLING STRENGTH OF CURVED I-GIRDER

(1) Lateral buckling strength

The lateral buckling stress σ_u of a curved I-girder can be obtained by dividing the ultimate moment M_u by the corresponding section modulus W_y as follows;

$$\sigma_u=M_u/W_y \qquad \cdots\cdots(12)$$

To simplify the expression for σ_u, let us now arrange σ_u by means of the following buckling parameter α which is defined by the Japanese Specification for Highway Bridges[3];

$$\alpha=2/\pi\cdot\sqrt{3+A_w/(2A_c)}\cdot(l/b)\sqrt{\sigma_y/E} \qquad \cdots\cdots(13)$$

in which

A_c; area of compression flange
A_w; area of web plate
b; width of compression flange

and the effective buckling length l can be written by;

$$l=\lambda L \qquad \cdots\cdots(14)$$

where L $(=R_s\Phi)$ is the span length of curved I-girder, and the coefficient λ can approximately be put as

$$\lambda=0.492\{1+0.035\Phi(L/b)^{1/3}\} \qquad \cdots\cdots(15)$$

through the parametric studies on the basis of elastic lateral buckling analysis[5].

Fig. 19 shows the relationships between σ_u/σ_y, α and Φ. The buckling stress σ_u is entirely depended upon the buckling parameter α and the central angle Φ of curved I-girder.

(2) Proposition of allowable bending compressive stress for curved I-girder

The allowable bending compressive stress $(\sigma_{ba})_c$ can be obtained by dividing the lateral buckling stress by the safety factor ν as follows;

$$(\sigma_{ba})_c=\sigma_u/\nu \qquad \cdots\cdots(16)$$

In order to express this stress by that of a straight I-girder $(\sigma_{ba})_s$, the reduction factor $\psi_1(\alpha, \Phi)$, which is the function of buckling parameter α and central angle Φ of curved I-girder, must be multiplied by $(\sigma_{ba})_s$, thus

$$(\sigma_{ba})_c=\psi_1(\sigma_{ba})_s \qquad \cdots\cdots(17)$$

This reduction factor $\psi_1(\alpha, \Phi)$ can be plotted as shown in **Fig. 20**, and can approximately be given by the following formula through the least square method within the ranges $0.1\leq\alpha\leq\sqrt{2}$ and $\Phi\leq0.2$[5].

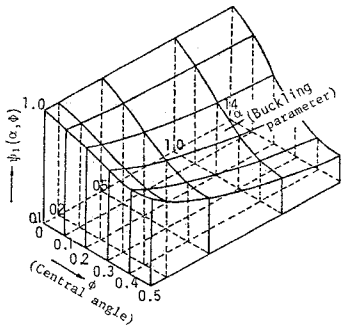

Fig. 20 Variations of $\psi_1(\alpha, \Phi)$.

$$\psi_1=1-1.05\sqrt{\alpha}(\Phi+4.52\Phi^2) \quad \cdots\cdots(18)$$

5. APPLICATION TO DESIGN OF MULTIPLE CURVED I-GIRDER BRIDGES

(1) Stress in main girders[26]

The stress bending in each main girder of a multiple curved I-girder bridge is given by

$$\sigma_b=M_y/I_y\cdot z \quad \cdots\cdots(19)$$

On the other hand, the additional warping stress σ_ω due to the out-of-plane bending of flange plates can be estimated by referring **Fig. 21** (a)~(c) as follows;

$$\sigma_\omega=\pm k\sigma_b/(RW_f)\cdot(A_f+A_s/3)L^2 \quad \cdots\cdots(20)$$

provided that the rigid supports are assumed at the junction points of floor beams or sway and lateral bracings, and where

A_f; cross-sectional area of flange plate, A_s; cross-sectional area of web plate from flange to neutral axis, L; longitudinal spacing of floor beams or sway and lateral bracings, R; radius of curvature of main girder, W_f; section modulus of flange plate ($=t_f b_f^2/6$, and t_f; flange thickness, b_f; flange width), k; bending moment coefficient as a continuous beam and can approximately be used $k=0.106$ as the maximum value.

(2) Check for stress and lateral buckling strength

The total compressive stresses at the compression flange of main girders should be satisfied the following criteria as defined by the specification;

$$\left.\begin{aligned}&\sigma_{bc}+\sigma_{\omega c}\leq\sigma_{ba0};\ \text{for stress check}\\&\sigma_{bc}\leq(\sigma_{ba})_c\quad;\ \text{for buckling check}\end{aligned}\right\} \quad \cdots\cdots(21)_{a,b}$$

where

σ_{bc}; bending compressive stress, $\sigma_{\omega c}$; additional warping compressive stress, σ_{ba0}; upper limit of allowable compressive stress $(\sigma_{ba})_c$; allowable compressive stress for lateral buckling.

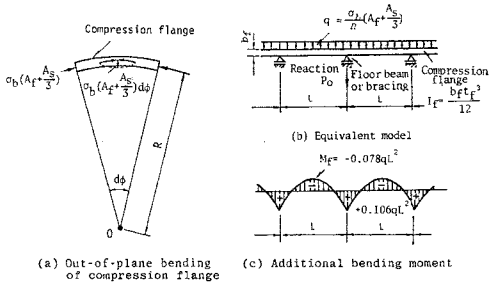

Fig. 21 Additional warping stress σ_ω.

It is, however, inconvenient for the practical use of simultaneous equations $(21)_{a,b}$. Then, dividing both sides of Eq. $(21)_a$ by σ_{ba0} and approximating the denominator of first term of left hand-side of this equation with $(\sigma_{ba})_c$, a simplified interaction formula can be obtained as follows;

$$\frac{\sigma_{bc}}{(\sigma_{ba})_c}+\frac{\sigma_{\omega c}}{\sigma_{ba0}}\leq 1.0 \quad \cdots\cdots(22)$$

i.e. Eq. $(21)_b$ can entirely be fulfilled when $\sigma_{\omega c}=0$, and gives safety side when $\sigma_{\omega c}=0$.

Fig. 22 shows the interaction curves for σ_{bc}/σ_{ba0} vs. $\sigma_{\omega c}/\sigma_{ba0}$ and $(\sigma_{ba})_c/\sigma_{ba0}$ vs. $\sigma_{\omega c}/\sigma_{ba0}$, respectively.

Note that the buckling modes of curved I-girders between the supported portions by the floor beams or sway and lateral bracings have the same modes as the straight I-girder, when the central angle Φ is sufficiently small. This condition has been inquired from various parametric analyses, which gives $\Phi\leq 0.02\alpha$. For these curved girders, the criterion relative to the straight girder can be applied to that of the curved girder by putting $\lambda=1$.

For the composite girder, the stress check can be conducted by Eq. $(21)_a$ alone. Moreover, the stress check for the tension flange can, of course, be conducted by;

$$\sigma_{bt}+\sigma_{\omega t}\leq\sigma_{ta} \quad \cdots\cdots(23)$$

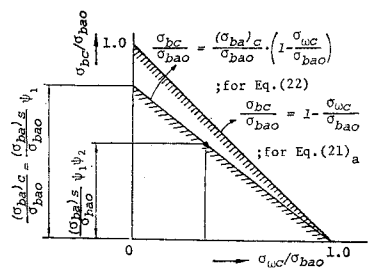

Fig. 22 Interaction curves for compression flange due to bending and additional warping stresses.

Now, Eq. (22) can be rewritten as follows;

$$\sigma_{bc} \leq (\sigma_{ba})_c (1-\sigma_{wc}/\sigma_{ba0}) \quad \cdots\cdots(24)$$

Then, substitution of Eq. (17) into the above equation gives

$$\sigma_{bc} \leq (\sigma_{ba})_s \psi_1 \psi_2 \quad \cdots\cdots(25)$$

where

$$\psi_2 = 1-\sigma_{wc}/\sigma_{ba0} = 1-(\sigma_{bc}/\sigma_{ba0})\cdot(\sigma_{wc}/\sigma_{bc}) \quad \cdots\cdots(26)$$

This equation is similar to a recommendation to AASHTO specification[27].

6. DESIGN METHOD OF FLOOR BEAMS, SWAY AND LATERAL BRACINGS FOR MULTIPLE CURVED I-GIRDER BRIDGES

The multiple curved girder bridges, which are stiffened by the floor beams or sway and lateral bracings, always undergo the additional stresses due to the curvature of a bridge axis. These stresses are thought to be the primary ones rather than the secondary stresses in the straight girder bridges, then the floor beams or sway and lateral bracings should be designed so as to have enough strength and rigidities as the following manners in which informations are derived from the references 2) and 26)~31).

(1) Floor beams or sway bracings

The necessary rigidity for the floor beams or sway bracings will be estimated by a condition given by the grillage theory as follows[31];

$$z=(l/2a)^3\cdot(I_Q/I)\geq 10 \quad \cdots\cdots(27)$$

where l; span length of multiple curved I-girder bridge, a; spacing of main girder, I, I_Q; moment of inertia of main girder and floor beam or sway bracing, respectively.

According to a recommendation for AASHTO specification[27], the adequate spacing of floor beams or sway bracings can be determined in connection with the radius of curvature R of the multiple curved I-girder bridge.

(2) Lateral bracings[2]

The lateral bracings should be attached to the upper and lower side of the flanges of the multiple curved I-girder bridges in order to decrease the additional stresses in the flange plates and to have the stability against overall lateral buckling of bridges during the erection[28]~[29].

The strength of lateral bracing against horizontal forces such as wind or seismic loads should not only be taken into consideration, but also the following check must be performed for the multiple curved I-girder bridges.

a) Additional stress due to out-of-plane bending of flange plates

The following reaction P_0 will be applied to the lateral bracings at the junction points of the main girders as already shown in **Fig. 21** (b).

$$P_0=\frac{\sigma_b(A_f+A_s/3)}{R}\cdot\frac{l_1+l_2}{2} \quad \cdots\cdots(28)$$

where l_1, l_2; spacing of lateral bracing as shown in **Fig. 23**.

The resulting stresses caused by this reaction P_0 can easily be found by referring **Fig. 23** as follows;

$$\left.\begin{aligned}\sigma_1&=P_0/A_1\cdot\sin\theta_2/\sin(\theta_1+\theta_2)\\ \sigma_2&=P_0/A_2\cdot\sin\theta_1/\sin(\theta_1+\theta_2)\end{aligned}\right\} \quad \cdots\cdots(29)$$

where

σ_1, σ_2; normal stress

A_1, A_2: cross-sectional area

θ_1, θ_2; inclination angle

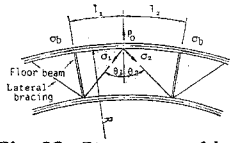

Fig. 23 Stress caused by out-of-plane bending of flange plate.

b) Additional stress due to torsion

The multiple curved I-girder bridges are always subjected to the torsional moment. The stress due to torsion can approximately be evaluated by the following simplified method. First, let a multiple curved girder bridge be idealized as a quasi-box bridge[30]. The equivalent thickness t_r of top or bottom plates of those box girder bridge can be reduced as follows;

$$t_r=\frac{E}{G}\cdot\frac{al}{(d^3/A_d+2l^3/3A_f)} \quad \cdots\cdots(30)$$

where A_d; cross-sectional area of lateral bracing, A_f; cross-sectional area of flange plate, a; spacing of main girder, d; length of lateral bracing, l; spacing of lateral bracing, E; Young's modulus, G; shear modulus of elasticity (see **Fig. 26**).

Fig. 24 illustrates the corresponding quasi-box girder bridges.

Next, the shear flow q due to the torsional moment T can be estimated by Bredt's formula as follows;

$$q=T/2F \quad \cdots\cdots(31)$$

where the torsional moment can approximately

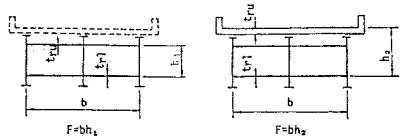

(a) Non-composite girder (b) Composite girder

Fig. 24 Quasi-box girder bridges.

Table 3 Torsional moment T.

Loads	Loading position	Formulae for torsional moment	Interporation at intermediate span
Dead load	Edge-span	$T_{d1}=W_d R^2\left(\frac{1-\cos\Phi}{\sin\Phi}-\frac{\Phi}{2}\right)$	parabolic curve $T_{d2}=0$
	Mid-span	$T_{d2}=0$	
Live load		$T_{l1}=P_l(R_p-R)+q_l R_p\left(R_p\frac{1-\cos\Phi}{\sin\Phi}-\frac{R\Phi}{2}\right)$	parabolic curve
		$T_{l2}=\frac{P_l}{2}(R_p-R)+\frac{q_l R_p}{4}\left(R_p\frac{1-\cos\Phi}{\sin\Phi}-\frac{R\Phi}{2}\right)$	

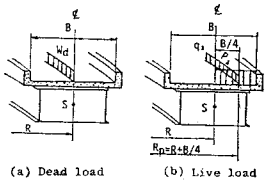

Fig. 25 Loading conditions.

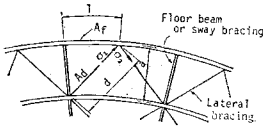

Fig. 26 Additional stress caused by torsion.

be determined by **Table 3** corresponding to the loading conditions as shown in **Fig. 25**[2].

Finally, hence the force acts on the lateral bracing with the length d is

$$Q=qd \quad \cdots\cdots(32)$$

the normal stresses due to torsion can be estimated by

$$\left.\begin{aligned}\sigma_1=-Q/A_1;&\ \text{compression}\\ \sigma_2=Q/A_2;&\ \text{tension}\end{aligned}\right\} \quad \cdots\cdots(33)$$

and plotted as shown in **Fig. 26**.

7. CONCLUSION

This paper deals with the lateral buckling strength and corresponding rational design method of the horizontally curved I-girder bridges.

Through the experimental studies on multiple curved I-girder models, it is shown that the overall lateral buckling is not so important phenomenon that the local buckling of main girder between the supported portions by floor beams or sway and lateral bracings should be taken into accounts for designing the curved I-girder bridges.

Accordingly, the local buckling tests of twenty seven model girders were carried out under the loading conditions of approximately pure bending. Then, numerous data could be obtained to estimate the buckling strength of curved I-girder.

On the other hand, the analytical method to evaluate the lateral buckling strength of curved I-girders was discussed in connection with the experimental data. The fundamental equation by using the second order analysis can be derived by taking into consideration both the geometrical and material non-linearities. It seems that the theoretical values coincide well with the experimental ones in the case where the central angle of girder is $\Phi \leq 0.2$ rad.

Then, the ultimate strength for lateral buckling was investigated through the buckling parameter α and the central angle Φ of curved I-girder. And, the applications of these results to the design of multiple curved I-girder bridges can be shown in detail, and a simplified interaction curve can be proposed, which is the similar form as a recommendation for AASHTO specification.

Finally, the design methods of floor beams or sway and lateral bracings to prevent the overall lateral buckling and to have enough strength and rigidities against additional stresses due to out-of-plane bending of flange plate and torsional moment can concretely be indicated in this paper.

8. ACKNOWLEDGEMENTS

The authors heartly wish to acknowledge the valuable suggestions given by Prof. S. Komatsu of Osaka University. Our thanks are also due to; The Japanese Ministry of Education for Scientific Research Funds and the sponsorship by the Hanshin-Highway Public Corporation.

REFERENCE

1) The Task Committee on Curved Box Girders of the ASCE-AASHTO Committee of Metal of ASCE Structural Division: Curved Steel Box-Girder Bridge: A Survey, Proc. of ASCE, ST-11, pp. 1697～1718, Nov., 1978.
2) The Hansin Highway Public Corporation: The Design Code, Part 2, Design codes for structure, April, 1980 (in Japanese).
3) The Japanese Road Association: The Japanese Specification for Highway Bridges, Feb., 1980.
4) Kotoguchi, H., H. Nakai and M. Kubo: Stiffening effects of sway and lateral bracings upon the ultimate strength of curved I-girder bridges, 33th Annual Conference of JSCE, pp. 131～132, Sept., 1978 (in Japanese).
5) Kotoguchi, H., M. Kubo and H. Nakai: Study on Geometric Non-linearity of Thin-Walled

Horizontally Curved Beams and Application to Lateral Buckling Strength of Curved I-Beams, 24th Structural Symposium of Non-linear Problem for Structure, pp. 69~76, Feb., 1978 (in Japanese).
6) Love, A. E. H.: Mathematical Theory of Elasticity, 4th. ed., Cambridge Press, 1952.
7) Namita, Y.: Die Theorie II. Ordnung von Krummten Stäben und ihre Anwendung auf das Kipp-Problem des Bogenträgers, Trans. of JSCE, No. 155, s. 87~103, 1970.
8) Ojalvo, M., E. Demutu and F. Takarz: Out-of-plane Buckling of Curved Members, Proc. of ASCE, Vol. 95, ST-11, pp. 2305~2316, Nov., 1969.
9) Tameroglu, S. and I. Turkey: Finite Theory of Thin Elastic Rods, Acta Mechanica, 11, pp. 271~282, 1971.
10) Schroeder, F. H.: Allegemine Stabtheorie des raumlich Vorgekrümungen und Vorgewunden Trägers mit Grossen Verformungen, Ing-Archiv. 39, s. 87~103, 1970.
11) Enda, Y.: Analysis of Thin-Walled Curved Beams with Open Cross Section as Finite Displacement Theory by Transfer Matrix Method, Proc. of JSCE, No. 199, pp. 11~20, May, 1972 (in Japanese).
12) Usuki, M., T. Kano and N. Watanabe: Analysis of Thin Walled Curved Members in Account for Latge Torsion; Proc. of JSCE, No. 290, pp. 1~12, Oct., 1979 (in Japanese).
13) Hirashima, M., M. Iura and T. Yada: Finite Displacement Theory of Naturally Curved and Twisted Thin-Walled Members, Proc. of JSCE, No. 292, pp. 13~25, Dec., 1979 (in Japanese).
14) Nakai, H., S. Muramatsu, N. Yoshikawa, T. Kitada and R. Ohminami: A Survey for Web Plates of the Horizontally Curved Girder Bridges, Bridge and Foundation, pp. 38~45, May, 1981.
15) Culver, C. G. and P. F. McManus: Instability of Horizontally Curved Members-Lateral Buckling of Curved Plate Girder, Carnegie-Mellon Univ. Report, Sept. 1971.
16) McManus, P. F.: Lateral Buckling of Curved Plate Girders, Ph. D. Disertation, Department of Civil Engineering, Canegie-Mellon University, 1971.
17) Fukumoto, Y. and S. Nishida: Ultimate Load Behavior of Curved I-Beams, Proc. of ASCE, Vol. 107, EM-2, pp. 367~388, 1981.
18) Clark, J. W. and J. R. Jambock: Lateral Buckling of I-Beams Subjected to Unequal End Moments, Proc. of ASCE, Vol. 83, EM-3, July, 1957.
19) Galambos, T. V.: Inelastic Buckling of Beams, Proc. of ASCE, Vol. 89, ST-5, Oct. 1963.
20) Column Research Council: Guide to Design Criteria for Metal Compression Members, John Wiley and Sons, New York, 1966.
21) Galambos, T. V.: Structural Members and Frames, Prentice Hall, Inc., 1968.
22) Structural Stability Research Council: Guide to Stability Design Criteria for Metal Structures, 3rd. Ed., John Wiley & Sons, 1976.
23) Fukumoto, Y., M. Fujiwara and N. Watanabe: Inelastic Lateral Buckling Tests on Welded Beams and Girder, Proc. of JSCE, No. 189, pp. 39~51, May, 1971 (in Japanese).
24) Nakai, H., H. Kotoguchi and T. Tani: Matrix Structural Analysis of Thin-Walled Curved Girder Bridges Subject to Arbitrary Loads, Proc. of JSCE, No. 225, pp. 1~15, Nov. 1976 (in Japanese).
25) Maegawa, K. and H. Yoshida: Ultimate Strength Analysis of Curved I-Beams by Transfer Matrix Method, Proc. of JSCE, No. 312, pp. 27~42, Aug., 1981 (in Japanese).
26) Nakai, H. and C. P. Heins: Analysis Criterion for Curved Bridges, Proc. of ASCE, ST-7, pp. 1419~1427, July, 1977.
27) The Task Committee on Curved Girders of the ASCE-AASHTO Committee on Flexual Member of the Committee on Metals of Structural Division: Curved I-Girder Bridge Design Recommendations, Proc. of ASCE, Vol. 103, ST-5, pp. 1137~1167, May, 1977.
28) Otsuka, H. and T. Yoshimura: Studies on Additional Stresses of Main Girders and Member Forces of Lateral Bracing in Curved I and Straight I-Girder Bridges, Proc. of JSCE, No. 290, pp. 17~29, Oct., 1979 (in Japanese).
29) Otsuka, H., T. Yoshimura, H. Hikosaka and K. Hirata: Analysis of Curved Girder Bridges Considering Eccentric Connection Between a Deck Plate and Girders, Proc. of JSCE, No. 259, pp. 11~23, May, 1977 (in Japanese).
30) Heins, C. P.: Bending and Torsional Design in Structural Members, Lexington Book, 1975.
31) Komatsu, S., H. Nakai and Y. Taido: A proposition for Designing the Horizontal Curved Bridges in Connection with Ratio between Torsional and Flexural Rigidities, Proc. of JSCE, No. 224, pp. 55~66, Apr., 1974 (in Japanese).

(Received December 20, 1982)

土木学会論文報告集　第339号

曲線Ｉ桁橋の横倒れ座屈強度と設計法に関する研究

（中井　博／事口寿男）

昭和58年11月

比較的スパンの短い鋼曲線桁橋では，製作が容易で経済性の発揮できるＩ桁橋が建設される機会が多く，今後もその需要はますます増加するものと思われる．しかしながら，わが国の道路橋示方書においては，曲線Ｉ桁橋の横倒れ座屈に関した基準が設けられておらず，直線Ｉ桁橋の規定を準用しているのが現状である．一方，米国では1977年米国土木学会の鋼構造委員会が曲線Ｉ桁橋の横倒れ座屈に関する照査方法を示した．それによると，曲線Ｉ桁橋の横倒れ座屈に関する基準は，直線Ｉ桁橋に関するものよりもかなり厳しくなっており，わが国でも曲線Ｉ桁橋の横倒れ座屈に対し十分な安定性を確保した設計を行う必要があると思われる．

本研究では，まず実橋をモデルとした並列曲線Ｉ桁橋の３体の全体模型桁による耐荷力実験を実施した結果，横桁，あるいは対傾構，および横構が十分に剛であれば，その固定点間距離内での各主桁の横倒れ座屈挙動が並列曲線Ｉ桁橋の崩壊につながることが明らかとなった．また，曲線Ｉ桁橋の固定点間距離内の主桁の横倒れ座屈モードは，直線Ｉ桁橋のものと異なることが明らかとなった．

したがって，次に曲率半径，スパン，および道路橋示方書で与えられている座屈パラメーターαが種々異なる27体のＩ形模型による横倒れ座屈実験を，実橋をモデルにした境界条件を用いて行った．その結果，曲線Ｉ形ばりの中心角と座屈パラメーターαが大になれば，横倒れ座屈強度は低下することが明らかとなった．

一方，材料，および幾何学的非線形性を考慮した２次理論によって曲線Ｉ形ばりの横倒れ座屈強度を数値計算した．曲線Ｉ形ばりの中心角が0.2 rad以内では実験値と理論値との比は90%～110%にあり，両者はよく一致した．

これらの実験値，および理論値より，まず並列曲線Ｉ桁橋の固定間距離内における主桁の有効座屈長の算定式を示し，曲線Ｉ形ばりの横倒れ座屈強度式を中心角Φと座屈パラメーターαによって整理した．さらに，並列曲線Ｉ桁橋の主桁設計への適用に際し，簡単な相関曲線によって，横倒れ座屈を考慮した応力照査式を提示した．

並列曲線Ｉ桁橋では，通常，荷重分配作用の増大と橋全体のねじり剛性を高めるために十分な剛性を有する横桁，あるいは対傾構，および横構を配置しなければならない．したがって，これらの横桁，あるいは対傾構，および横構を合理的に設計するための指針を与えた．すなわち，横桁，あるいは対傾構に対し，その必要剛度の算定式を示した．また，風荷重や地震荷重以外で，曲率の影響によるフランジに作用する面外方向応力とねじりモーメントによって生じる横構部材応力の算定法を示した．